Adaptive Multitherapy for HIV Infection

Pedro Vasco
pedro.vasco@tecnico.ulisboa.pt

Instituto Superior Técnico, Lisboa, Portugal

November 2019

Abstract

This work focuses on the adaptive control of HIV infection when the treatment is done using multitherapy. A nonlinear three-variable model is used on which a study of the dynamics and linearizations is made. The purpose of the controllers will be to bring the number of free virions to a certain reference value, lower than the detection thresholds of the current instruments. Two therapies are used simultaneously (RTI and PI) and the control variable is related to the effect values of the therapies. Initially, a non-adaptive approach is used in which different types of controllers are tested and their performance compared. At this point it is considered that a prior knowledge of the parameters of the system is available. Subsquently, an approach in which two different adaptation mechanisms is used in conjunction with different controllers to evaluate which strategy produces the better results. The inclusion of adaptation allows to deal with the great variability among patients, as cases with greater and lesser initial uncertainty are tested. The different cost functions used in controllers are designed such that, in equilibrium, the values of the two different therapies are similar, thereby minimizing toxicity.

Keywords: HIV infection control, adaptative control, model predictive control, biomedical systems, multiple switched models, pcertainty equivalence principle

1. Introduction

1.1. Motivation

AIDS is a disease that affects the immune system, caused by the HIV virus. AIDS is not itself a deadly disease. However, by weakening the immune system, it leads to other types of diseases, which in a healthy individual would be easily controlled, to potentially be deadly.

Nowadays there is a set of drugs that are very effective in controlling the disease, even leading to an infected individual having a nearly 0% chance of transmitting the virus when properly medicated. However this type of medication requires extremely regular dosing which causes undesirable side effects. This work gains special relevance because through existing models it is possible to determine optimal therapy doses, controlling the virus and reducing the adverse effects of therapy.

1.2. Literature review

In [4], [5], [7], [13] and [17] different models of HIV infection with and without therapy effects are described being that in [14] and [22] the pharmacokinetic and pharmacodynamic models are also described. In [6] there is a description of the different therapies.

In [6], [9], [12], [20] different strategies to control the HIV infection using optimal control are shown and in [8], [14], [18], [19] and [23] strategies using predictive control are shown.

In [2] and [3] it can be found a description of the certainty equivalence principle and in [10] and [15] it can be found a description of the multiple model switching.

2. Dynamic Model of HIV Infection

The model of HIV infection that will be studied in detail is

$$\begin{cases} \dot{T} = s - dT - \beta T v \\ \dot{T^*} = \beta T v - \mu_2 T^* \\ \dot{v} = kT^* - \mu_1 v \end{cases}, \tag{1}$$

where T represents healthy T CD4+ cells, T^* infected T CD4+ cells and v the number of free virions.

This model has two equilibrium points. One corresponding to the absence of infection

$$\begin{bmatrix} \bar{T_1} \\ \bar{T_1^*} \\ \bar{v_1} \end{bmatrix} = \begin{bmatrix} \frac{s}{d} \\ 0 \\ 0 \end{bmatrix}, \tag{2}$$

and another corresponding to the asymptomatic phase of the infection

$$\begin{bmatrix} \bar{T}_2 \\ \bar{T}_2^* \\ \bar{v}_2 \end{bmatrix} = \begin{bmatrix} \frac{\mu_1\mu_2}{\beta k} \\ \frac{s}{\mu_2} - \frac{d\mu_1}{\beta k} \\ \frac{ks}{\mu_1\mu_2} - \frac{d}{\beta} \end{bmatrix}. \quad (3)$$

Typical values for model parameters are shown in Table 1.

t	Days
d	0.02 per day
k	100 per cell
s	10 mm^{-3} per day
β	$2.4 \times 10^{-5} mm^{-3}$ per day
μ_1	2.4 per day
μ_2	0.24 per day

Table 1: Typical values for model parameters.

In case of absence of infection, whatever the initial T value, it will always evolve into equilibrium. The T^* and v variables remain at zero as expected because there is no infection.

Otherwise, when there is infection, it can be concluded that whatever the initial conditions of T and v are, the system always evolves to an equilibrium point corresponding to the asymptomatic phase. However, the way it progresses to this point differs depends on the initial conditions, namely the time it takes to reach this point.

After being infected, the individual reaches a virion peak at the same time as the number of healthy cells drop dramatically. After reaching this peak, the number of virions decreases again and the number of healthy cells increases due to the immune system response to the infection.

Figure 1 shows the state-space representation of the system.

Whatever the initial condition is, the system always converges to the equilibrium point, so, it can be concluded that the equilibrium point is stable.

2.1. Model With Therapy

The HIV model, including therapy effects of RTI and PI, is given by

$$\begin{cases} \dot{T} = s - dT - (1-u_1)\beta T v \\ \dot{T^*} = (1-u_1)\beta T v - \mu_2 T^* \\ \dot{v} = (1-u_2)kT^* - \mu_1 v \end{cases}. \quad (4)$$

Different simulations were made applying each one of the therapies individually and both simultaneously. By combining the two therapies, it is possible to achieve the same results as with using them individually but using smaller quantities. In the case of multitherapy, making $u_1 = 0.3$ and $u_2 = 0.4$ achieves roughly the same effects as using just one with 0.5 or more.

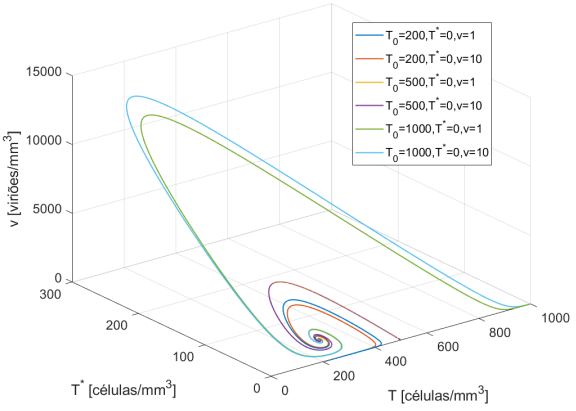

Figure 1: State-space representation.

2.1.1 Linearization

The system linearization allows to study its behavior for small deviations around the equilibrium point.

The behavior of a system around an equilibrium point can be described by the following state space representation:

$$\frac{d}{dt}\Delta x(t) = A\Delta x(t) + B\Delta u(t). \quad (5)$$

In order to obtain the dynamic matrix of the linearized system, each of the model equations (4) has to be derived in respect to the three different states.

The linearized dynamic matrix around a generic equilibrium point $(\bar{T}, \bar{T^*}, \bar{v})$ is

$$A = \begin{bmatrix} -d - \beta\bar{v} & 0 & -\beta\bar{T} \\ \beta\bar{v} & -\mu_2 & \beta\bar{T} \\ 0 & k & -\mu_1 \end{bmatrix}. \quad (6)$$

The dynamic matrix around the asymptomatic phase equilibrium point (3) is

$$A = \begin{bmatrix} -\frac{\beta ks}{\mu_1\mu_2} & 0 & -\frac{\mu_1\mu_2}{k} \\ \frac{\beta ks}{\mu_1\mu_2} - d & -\mu_2 & \frac{\mu_1\mu_2}{k} \\ 0 & k & -\mu_1 \end{bmatrix}. \quad (7)$$

The B matrix is given by

$$B = \begin{bmatrix} \frac{\delta f_1}{\delta u_1} & \frac{\delta f_1}{\delta u_2} \\ \frac{\delta f_2}{\delta u_1} & \frac{\delta f_2}{\delta u_2} \\ \frac{\delta f_3}{\delta u_1} & \frac{\delta f_3}{\delta u_2} \end{bmatrix} = \begin{bmatrix} \beta\bar{T}\bar{v} & 0 \\ -\beta\bar{T}\bar{v} & 0 \\ 0 & -k\bar{T^*} \end{bmatrix}. \quad (8)$$

The dynamic matrix B around the asymptomatic

phase equilibrium point (3) is

$$B = \begin{bmatrix} s - \frac{d\mu_1\mu_2}{\beta k} & 0 \\ \frac{d\mu_1\mu_2}{\beta k} - s & 0 \\ 0 & \frac{d\mu_1}{\beta} - \frac{ks}{\mu_2} \end{bmatrix}. \quad (9)$$

2.2. Model Discretization

Some types of controllers, such as the MPC controller, use discrete models, so it is necessary to determine the equivalent discrete model in order to use this type of controllers.

The linearized model is given by:

$$\begin{cases} \dot{x}(t) = Ax(t) + Bu(t) \\ y(t) = Cx(t) \end{cases} \quad (10)$$

This model corresponds to the discrete model given by:

$$\begin{cases} x(k+1) = \phi x(k) + \Gamma u(k) \\ y(k) = Cx(k) \end{cases} \quad (11)$$

with,

$$\phi = e^{Ah} \quad , \quad \Gamma = \int_0^h e^{A\sigma} d\sigma \cdot B. \quad (12)$$

The non-linear continuous model is given by

$$\begin{cases} \dot{x} = f(x,u) \\ y = Cx \end{cases} . \quad (13)$$

With the 4th order Runge-Kutta method, it is possible to approximate the continuous model by a discrete model given by:

$$\begin{aligned} x(k+1) &= x(k) + \frac{h}{6}(k_1 + 2k_2 + 2k_3 + k_4) \\ k_1 &= f(x(k)) \\ k_2 &= f(x(k) + \frac{h}{2}k_1) \\ k_3 &= f(x(k) + \frac{h}{2}k_2) \\ k_4 &= f(x(k) + hk_3), \end{aligned} \quad (14)$$

with a sample time h.

On the other hand, Euler method uses a simpler formulation given by:

$$x(k+1) = x(k) + hf(x(k), u(k)). \quad (15)$$

By simulation, it can be stated that the Euler approximation introduces an approximation error in the representation of the infection model. On the other hand, the 4th order Runge-Kutta approximation leads to a faithful representation of the continuous model, introducing no observable error in the model representation.

3. Non Adaptative Control

In this subsection three types of controllers will be studied, so that by imposing a given reference on the value of v, it is possible to determine how much effect of the therapies need to be applied. For this, the system output is compared with the reference value, generating an error value. Given this error value, a certain amount of therapy will be applied so that over time the error tends to zero.

3.1. PI Controller

The proportional integral controller (PI) contains a proportional part and another part with an integrative effect. The proportional part is a simple K_p gain that multiplies the error generating a u_p value. The integrator will integrate the error so that when the tracking error is zero the control is non-zero. The integrator will also be associated with a gain called the integral gain (K_i).

To avoid controller spikes when the reference is a constant, it is defined a reference with exponential decay given by,

$$r = 877e^{0.05(300-t)} + 15, \quad (16)$$

that is, the reference now tends asymptotically to 15 and when control is turned on, at the moment $t = 300$, it has the same value as the current number of system virions. Controller gains are

$$K_{p1} = 0.10, K_{i1} = 1.01, K_{p2} = 0.10, K_{i2} = 13.00. \quad (17)$$

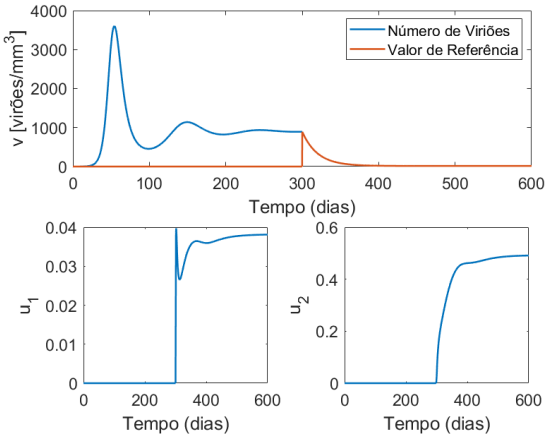

Figure 2: PI controller response for reference 15 with exponential decay.

By analyzing Figure 2 it can be concluded that the controller has a smooth response without taking excessively high values of control. The reference value is also followed.

3.2. LQ Controller

The PI controller does not minimize the usage of therapy so a different approach will be used through the LQ controller.

A cost function to be minimized is defined, given by

$$J = \int (x^T Q x + R u^2) dt. \tag{18}$$

The controller will contain an observer which will estimate the actual system state and then calculate the control to apply to the system. The observer's state model will be given by

$$\begin{cases} \dot{\hat{x}} = A\hat{x} + Bu + L(y - C\hat{x}) \\ u = -K\hat{x} \end{cases}. \tag{19}$$

The values of L and K are determined using the $lqr()$ and $lqe()$ functions of *MATLAB* respectively, taking into account the values defined for Q and R in the cost function. The L vector values will be calculated using the original observer model, however, as an integrator will be included in the controller, the matrix used to calculate the K gains will have to be an augmented matrix in order to obtain the gain of the integrator. The state model will then be

$$\begin{bmatrix} \dot{\hat{x}} \\ \dot{x}_i \end{bmatrix} = \begin{bmatrix} A & 0 \\ -\frac{C}{T_i} & 0 \end{bmatrix} \begin{bmatrix} \hat{x} \\ x_i \end{bmatrix} + \begin{bmatrix} B \\ 0 \end{bmatrix} u. \tag{20}$$

The control scheme can be described by the block diagram of Figure 3:

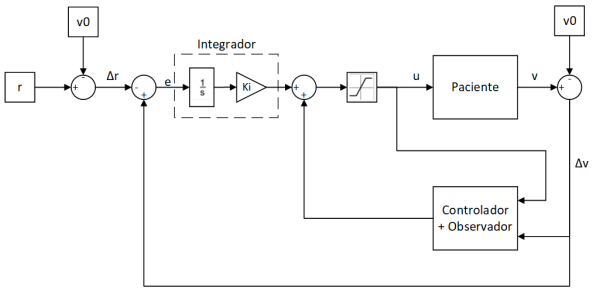

Figure 3: Block diagram of LQ controller.

The simulations start at the equilibrium point of the asymptomatic phase and the reference is given by

$$r(t) = 15 + 135 \cdot u_e(t-150) \cdot u_e(-t+300), t \geq 0. \tag{21}$$

By simulation it was concluded that the best values for R an Q are

$$R = 3.19 \cdot 10^5 \cdot \begin{bmatrix} 2 & 0 \\ 0 & 5 \end{bmatrix}, Q = \begin{bmatrix} 0 & 0 & 0 & 0 \\ 0 & 0 & 0 & 0 \\ 0 & 0 & 10 & 0 \\ 0 & 0 & 0 & 0.05 \end{bmatrix}. \tag{22}$$

The output of the system, the number of free virions, is now a noisy measure given by:

$$v_\eta(t) = v(t) + \eta(t) \ , \ \eta \sim \mathcal{N}(0, 10). \tag{23}$$

In these conditions the response of the controller is overly oscillatory. In order to solve that, the R value is now increased to

$$R = 3.19 \cdot 10^6 \cdot \begin{bmatrix} 2 & 0 \\ 0 & 5 \end{bmatrix}. \tag{24}$$

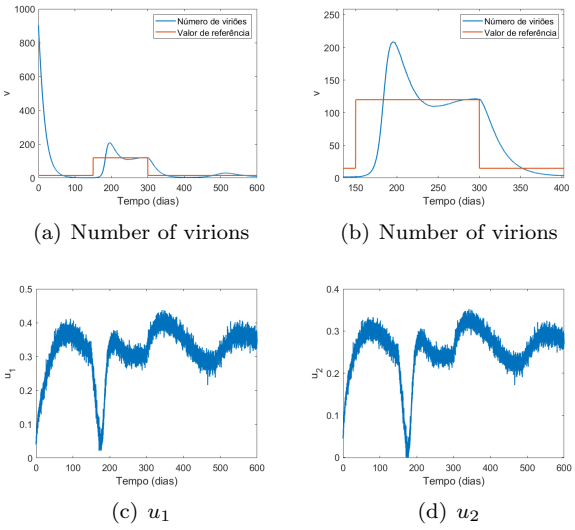

(a) Number of virions (b) Number of virions

(c) u_1 (d) u_2

Figure 4: Response of the multivariable LQ controller with reference change and noisy measure.

It is concluded by observing Figure 4 that increasing the value of R allows to mitigate the oscillatory character of the controller as expected. However, as was also predicted, the convergence to reference values becomes substantially slower.

3.2.1 Extended Kalman Filter

Given that the results using a linear observer demonstrate some problems, a different approach was used to estimate states using an extended Kalman filter [11].

The Kalman filter is a set of mathematical equations that provides an efficient recursive computational solution for the least squares method. The filter supports past, present, and future estimates, and can handle cases where noise or uncertainty exists in the modeled system.

Extended Kalman filter is used for processes described by nonlinear models. This type of filter calculates the estimates by linearizing around the current mean and covariance. At each instant the state and covariance estimates of the instant $k+1$ are calculated using the estimates of the instant k. These estimates are calculated according to:

$$\hat{x}_{k+1} = f(\hat{x}_k, u_k) \tag{25}$$

$$P_{k+1} = F_k P_k F_k^T + Q_{ek} \tag{26}$$

with Jacobian matrix F given by,

$$F_k = \frac{\partial f}{\partial x}|_{\hat{x}_k, u_k} = \begin{bmatrix} 1 - h(d + (1-u_1)\beta x_3) & 0 & -h(1-u_1)\beta x_1 \\ h(1-u_1)\beta x_3 & 1 - h\mu_2 & h(1-u_1)\beta x_1 \\ 0 & h(1-u_2)k & 1 - h\mu_1 \end{bmatrix}. \tag{27}$$

In order to prevent the existence of nonlinearities in the Jacobian matrix, the function f represents the approximation by the Euler method described in the equation (15) where f is given by:

$$\begin{cases} T(k+1) = T(k) + h(s - dT(k) - (1-u_1(k))\beta T(k) v(k)) \\ T^*(k+1) = T^*(k) + h((1-u_1(k))\beta T(k) v(k) - \mu_2 T^*(k)) \\ v(k+1) = v(k) + h((1-u_2(k))kT^*(k) - \mu_1 v(k)) \end{cases} \tag{28}$$

Then the estimates are recalculated using the new measurements. Kalman gain will be given by,

$$K_k = P_k H_k^T S_k^{-1} \tag{29}$$

with

$$H_k = \frac{\partial h_s}{\partial x}|\hat{x}_k = \begin{bmatrix} 1 & 1 & 0 \\ 0 & 0 & 1 \end{bmatrix} \text{and} S_k = H_k P_k H_k^T + R_{ek}. \tag{30}$$

The h function represents the function that defines the system output which in this case is given by:

$$h_s = \begin{bmatrix} T(k) + T^*(k) \\ v(k) \end{bmatrix}. \tag{31}$$

The new estimate of the state will be given by:

$$\hat{x}_k = \hat{x}_k + K_k \tilde{y}_k \tag{32}$$

where $\tilde{y}_k$ is the difference between the measured output value z_k and the predicted output value taking into account the estimate *a priori*. This error is given by,

$$\tilde{y}_k = z_k - h_s(\hat{x}_k). \tag{33}$$

The error covariance matrix is also recalculated according to

$$P_k = (I - K_k H_k) P_k. \tag{34}$$

The Kalman filter has 2 adjustable parameters. The matrix Q_e represents the process noise and the matrix R_e represents the measurement noise. The values of Q_e and R_e should be higher if the confidence about the values generated by the model and the measurements, respectively, is low. Similarly the initial values of P should be higher if the uncertainty about the initial measurements is high.

In this simulation the following adjustable parameters were used:

$$Q_e = \begin{bmatrix} 0.5 & 0 & 0 \\ 0 & 0.001 & 0 \\ 0 & 0 & 0.5 \end{bmatrix}, R_e = \begin{bmatrix} 100 & 0 \\ 0 & 100 \end{bmatrix}. \tag{35}$$

and

$$P_0 = \begin{bmatrix} 50000 & 0 & 0 \\ 0 & 100000 & 0 \\ 0 & 0 & 100000 \end{bmatrix}. \tag{36}$$

The parameter Q will have the same value as in (24) while R will be given by:

$$R = 5000 \cdot \begin{bmatrix} 1 & 0 \\ 0 & 8 \end{bmatrix} \tag{37}$$

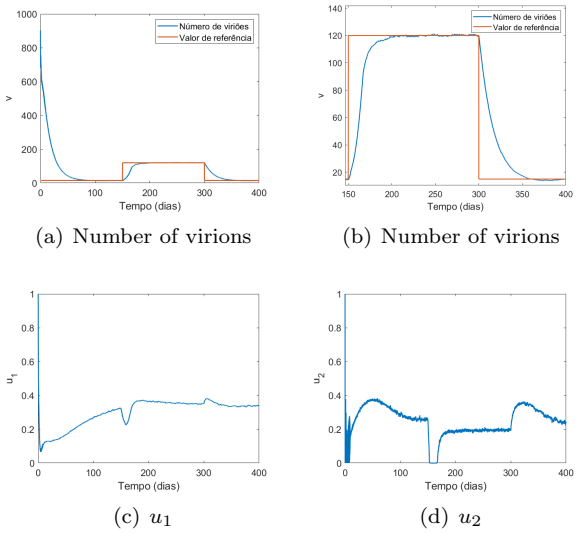

(a) Number of virions (b) Number of virions

(c) u_1 (d) u_2

Figure 5: Multivariable LQ controller response with state estimation by EKF.

From the analysis of Figure 5 it is concluded that the estimation of states through EKF rather than a linear observer leads to substantially better results. With this type of estimation the control is no longer excessively oscillating allowing the use of lower R values and consequently a faster controller response to reference variations.

3.3. MPC Controller

MPC control strategy is similar to the LQ controller in minimizing a cost function. However, here there is the ability to handle constraints. On the other hand, a non-quadratic cost function can be used. The optimization problem to solve is given by,

$$\begin{aligned} \underset{u}{\text{minimize}} \quad & J(k, k+H) = \sum_{i=1}^{H} (y(k+i) - r(k+i))^2 + \rho u^2(k-1) \\ \text{subject to} \quad & x(k+1) = f(x(k), u(k)), \\ & y(k) = Cx(k). \end{aligned} \tag{38}$$

This control strategy is a predictive control strategy, i.e., the controller predicts the system behavior taking into account the model that describes the system over a H size horizon. In order to follow the desired reference, the optimization problem is solved in order to u. Solving this optimization problem leads to a sequence of u values of size H. The first value of u is then applied to the system and the process is repeated. In order to ensure stability it is necessary to choose a sufficiently large H horizon.

3.3.1 NMPC Controller

According to [14] the toxicity of the different therapies has an exponential evolution. Taking this into account, the cost function to minimize will now be:

$$J(k, k+H) = \sum_{i=1}^{H} [(y(k+i) - r)^2 + \rho_1 \cdot (e^{\rho_2 \cdot u_1(k+i-1)} + e^{\rho_2 \cdot u_2(k+i-1)})]. \tag{39}$$

With this formulation it is assumed that the toxicity of both therapies (RTI and PI) has an equal evolution since the same parameter ρ_2 is used in both exponentials. The values for ρ_1 and ρ_2 are:

$$\rho_1 = 0.05 \ , \ \rho_2 = 15. \tag{40}$$

This type of approach leads to a slower convergence to the reference value, however it uses lower therapy values.

Since there is no direct access to the three different states an EKF is used to estimate them. The output measures are noisy measures given by:

$$\begin{cases} [T(k) + T^*(k)]_\eta = T(k) + T^*(k) + \eta(k) \\ v_\eta(k) = v(k) + \eta(k) \end{cases}, \tag{41}$$

where $\eta(k)$ follows a normal distribution with null average.

Firstly, it can be stated from Figure 6 that although the measurements are noisy, the Kalman filter can make the estimates converge to the real state value and therefore the controller can take the tracking error to 0. Comparing the differences in the existing noise power, the only difference lies in the state estimation which is slower for T and v.

Overall it can be said that the extended Kalman filter is a key tool for the control of the dynamic model of HIV because, in addition to allowing a precise estimation of the states, it allows measurement noise filtering.

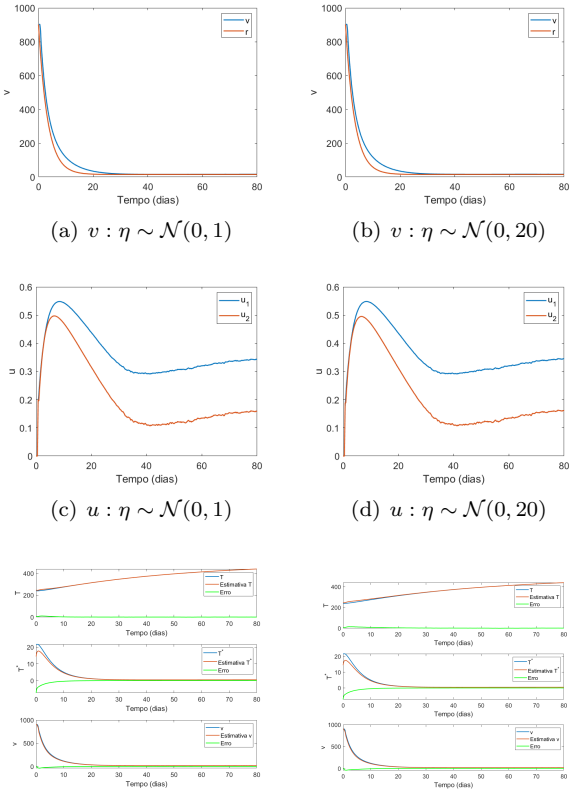

(a) $v : \eta \sim \mathcal{N}(0, 1)$ (b) $v : \eta \sim \mathcal{N}(0, 20)$

(c) $u : \eta \sim \mathcal{N}(0, 1)$ (d) $u : \eta \sim \mathcal{N}(0, 20)$

(e) Estimation: $\eta \sim \mathcal{N}(0, 1)$ (f) Estimation: $\eta \sim \mathcal{N}(0, 20)$

Figure 6: NMPC controller response with EKF and noisy measures.

4. Adaptative Control

Given the great variability of the patient during the evolution of infection and uncertainty of the built mathematical models, adaptation gains greater relevance. Adaptive methods allow to deal with patient variability by estimating models and recalculating controller gains based on collected patient data. This paper will discuss two different adaptation strategies.

4.1. Certainty Equivalence Principle

The certainty equivalence principle, taking into account input u and output y, estimates the model parameters using the least squares method. Then the controller gains are recalculated. The adaptive control type scheme can be represented by Figure 7.

As described in Figure 7, the control variable and the patient system output represent the inputs of the RLS block. This block will estimate the model parameters using the recursive least squares method. This variant of least squares estimates current system parameters using the previous estimate. Consider the system given by

$$y(k) = \varphi'(k-1)\theta + \eta(k). \tag{42}$$

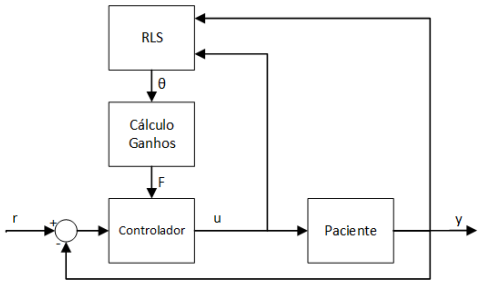

Figure 7: Certainty equivalence principle model.

The θ parameters are the parameters to estimate. Then the value of $\hat{\theta}$ will be given by

$$\hat{\theta}(k) = \hat{\theta}(k-1) + K(k)[y(k) - \varphi'(k-1)\hat{\theta}(k-1)], \quad (43)$$

with

$$P(k) = P(k-1) - \frac{P(k-1)\varphi(k-1)\varphi'(k-1)P(k-1)}{1 + \varphi'(k-1)P(k-1)\varphi(k-1)} \quad (44)$$

and

$$K(k) = P(k)\varphi(k-1) \quad (45)$$

After obtaining the parameters of the model, they are used to recalculate controller gains, with F being a vector of gains.

4.1.1 μ_1 Parameter Estimation

Consider that the μ_1 parameter, corresponding to virion mortality, is unknown and the remaining parameters are known. This parameter influences the evolution of the number of virions given by:

$$\begin{aligned} v(k+1) = v(k) + h((1 - u_2(k))kT^*(k) \\ - \mu_1 v(k)) + \eta(k) \ , \ \eta(k) \sim \mathcal{N}(0, 10). \end{aligned} \quad (46)$$

There is no direct acess to the three different states so an EKF was used. The EKF will estimate the states while the RLS block will estimate the μ_1 parameter. The representative block diagram of this scheme will be as follows:

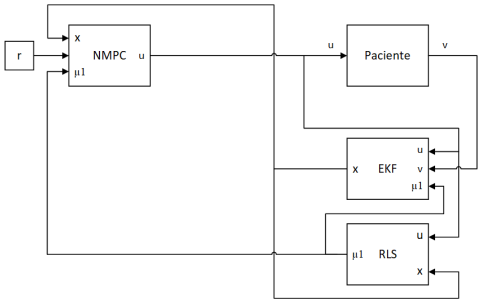

Figure 8: EKF+RLS block diagram.

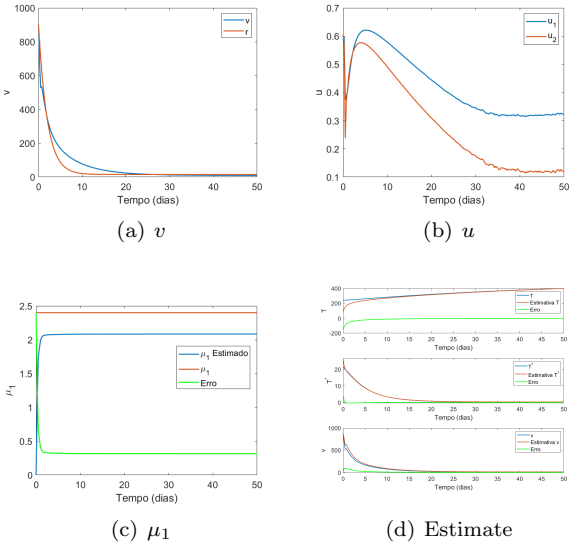

(a) v (b) u

(c) μ_1 (d) Estimate

Figure 9: Parallel EKF and RLS blocks.

By observing the simulation in Figure 9 we see that the estimate of μ_1 does not converge to the actual value. However, even with an incorrect value of μ_1, the Kalman filter can get state estimates to converge to the real value though at a slower rate than when the μ_1 value is known. This error in estimating μ_1 may be due to interdependence between blocks as EKF needs μ_1 to estimate states and the RLS block needs state value to estimate μ_1.

Since the simultaneous operation of the EKF and RLS blocks leads to parameter estimation error, a different approach has now been considered. The EKF block will now be an enlarged version of the previous one to estimate the states and the μ_1 parameter together. This eliminates the dependency between the two blocks. The vector to be estimated will now be a z vector given by,

$$z = \begin{bmatrix} x \\ \mu_1 \end{bmatrix} \quad (47)$$

given that

$$\begin{cases} \dot{x} = f(x, \mu_1) \\ \dot{\mu_1} = 0 \end{cases} . \quad (48)$$

As it can be seen on Figure 10, this enlarged version of the extended Kalman filter allows to take both state and parameter μ_1 estimation errors to zero and it is a better alternative to EKF and RLS blocks together described earlier. The existence of measurement noise means that the μ_1 estimation error is not exactly zero but fluctuates around zero over time.

Instead of an MPC controller an LQ controller can also be used. The extended EKF was used to estimate the states and the μ_1 parameter, similar

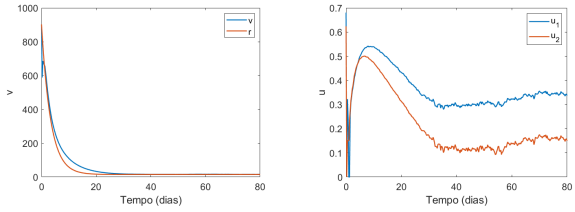

(a) v

(b) u

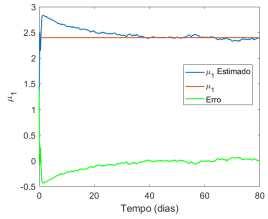

(c) μ_1

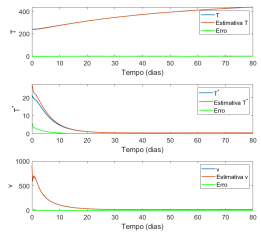

(d) Estimation

Figure 10: Enlarged EKF block.

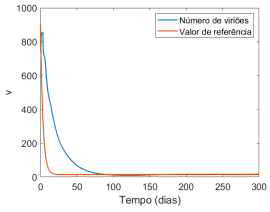

(a) v

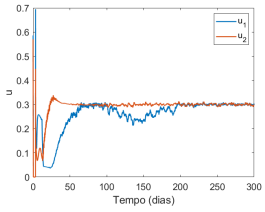

(b) u

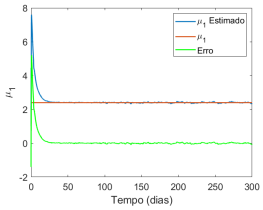

(c) μ_1

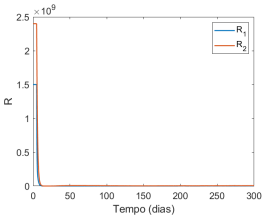

(d) R

Figure 12: Adaptive control using LQ controller and enlarged EKF with dynamic R.

to what had been done with the NMPC controller. Now it will no longer be necessary for the controller to estimate the states through the observer because it can use the estimations obtained by the EKF. Then at each instant of time the K vector gains are recalculated using the current μ_1 estimate. The block diagram of this new control strategy is given in Figure 11.

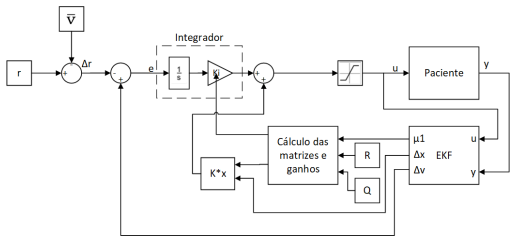

Figure 11: Block diagram of adaptive LQ controller with enlarged EKF.

In order to avoid controller saturation in the initial moments, a varying therapy weight was considered. R will now be ajusted at each sample interval by

$$R(k) = R(k-1)(1 - \gamma(c^2 - u^2)). \qquad (49)$$

From Figure 12 it can be seen that the estimation of μ_1 converges to the actual value. When compared to the case where the NMPC controller was used, the convergence time for the reference value is much longer.

4.1.2 Six Parameters Estimation

Since we are dealing with a biological system, which varies from patient to patient, it is not possible to know at first the parameters of the model describing this system. In the 4.1.1 section, it was assumed that five of the six parameters were known, estimating only the μ_1 parameter, and this estimation produced the best results when done with EKF. That said the estimation of all six parameters of the model will be done using this method.

Since, over time, estimates come closer to the actual value this means that the process noise will be lower. That said, the Q_e matrix associated with process noise should contain smaller values when t increases. So when $t > 10$ the Q_e matrix will be multiplied by a scaling factor of $\frac{1}{t-9}$.

In order to evaluate the ability of the algorithm to approximate the estimates when there is great uncertainty, a simulation with initial values of the parameters with substantial error (minimum of 100 % error) was performed. The initial values for the different parameters are

$$\begin{bmatrix} k_0 \\ \mu_{10} \\ \beta_0 \\ \mu_{20} \\ d_0 \\ s_0 \end{bmatrix} = \begin{bmatrix} 250 \\ 0.001 \\ 1 \cdot 10^{-4} \\ 0.0001 \\ 0.0001 \\ 30 \end{bmatrix} \qquad (50)$$

Through simulation it is concluded that at an early stage the parameters converge, however, they start to diverge at a certain time. This divergence leads to an error of up to 15000% causing a spring effect on the number of virions resulting from an interruption of therapy. One of the possible causes for this is that the number of virions and hence the number of CD4 + T cells stabilize at a given value thus avoiding changes in the system that would allow parameter estimation (absence of system agi-

tation). The solution to this problem will be to stop the estimates. In this case, it was decided to stop the estimates at $t = 15$. Note that at this moment it is already noticeable the divergence of the parameters s and d, however is when it can be seen the smallest estimation error of the remaining 4 parameters. With this it is possible to bring the tracking error to zero because the MPC controller now has values of the parameters close to the real ones. However, the estimates do not converge to zero error but only to a low value (in the order of 10% error) and the control saturates in the initial moments. The results of this stopping situation are shown in Figure 13.

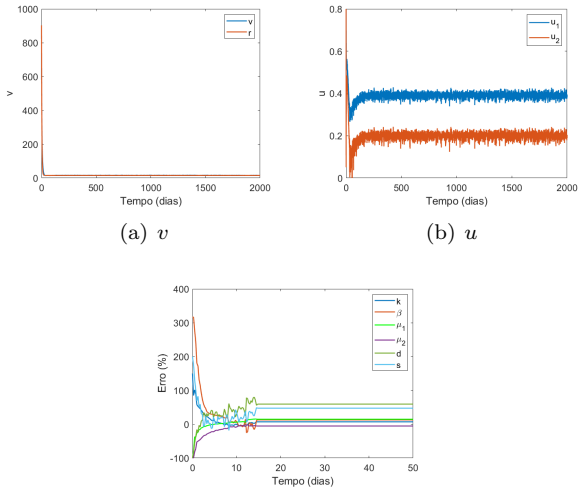

(a) v (b) u

(c) Error

Figure 13: Simulation with 6 parameter estimation by enlarged EKF.

4.2. Multiple Model Switching

The method of multiple model switching consists in having n different models. Let u be the input applied to the real system and y its output. This u input is then applied to the n models and the output of these $\hat{y_n}$ models is compared to the actual model output y. Since $e_n = ||y - \hat{y_n}||^2$, the model with the lowest value of e_n is chosen. Each of these models is associated with a given controller so when choosing one of these models, a new controller for the real system is also chosen. There is, however, a condition in choosing the model. If a certain model M_n and the associated controller C_n is chosen, it is neccessary to keep that C_n chosen for a minimum time interval. This residence time condition is necessary to ensure stability. The control scheme can be described by Figure 14. The *"Lógica de Escolha do Controlador"* block does not simply choose the model with the lowest mean square error. As stated above, there is a dwell time condition, which is guaranteed by this block. If there was fast switching the system could become unstable.

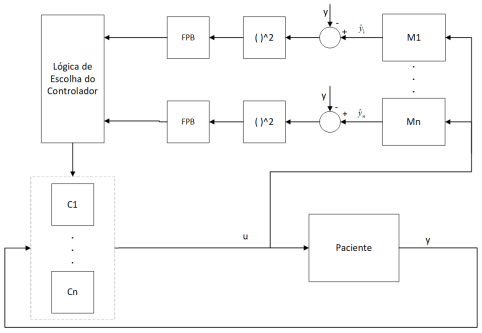

Figure 14: Block diagram of adaptive control with multiple model switching.

In order to use this adaptive control method 3 different models and their associated controller were considered. Each model corresponds to a linearization around a certain equilibrium point with the associated controller being an LQ controller designed accordingly. The controllers will be designed as described in section 3.2 with the A and B matrices depending on the model used. The Q and R weights in the cost function will be the same for the different models and given by:

$$R = 6.38 \cdot 10^6 \cdot \begin{bmatrix} 1 & 0 \\ 0 & 2 \end{bmatrix} \quad , \quad Q = \begin{bmatrix} 0 & 0 & 0 & 0 \\ 0 & 0 & 0 & 0 \\ 0 & 0 & 10 & 0 \\ 0 & 0 & 0 & 0.05 \end{bmatrix} \tag{51}$$

Model 1 corresponds to the linearization around the equilibrium point of the asymptomatic phase. Model 2 corresponds to linearization around the equilibrium point with $\bar{v} = 400$ and equal values of the two therapies. Model 3 corresponds to the linearization around the equilibrium point with $\bar{v} = 15$ and equal values of the two therapies.

The M_1 to M_n blocks represented in Figure 14 will in this case be Kalman filters with dynamics associated with the model they represent. The output y from the system will only be the number of virions and there will be measurement error $\eta \sim \mathcal{N}(0, 10)$. As shown in Figure 14 after comparing the models output and the actual value of v this signal is applied to a low pass filter to remove noise. This filter will be described by:

$$\pi(k) = \alpha\pi(k-1) + (1-\alpha)z(k), \tag{52}$$

where z is the signal at the exit of the squared error block and $\alpha = 0.99$. Switching between controllers leads to spikes in the control so the controllers integrator have been reset in each switch to avoid this problem. The gains associated with model 3 lead to oscillatory control so the gains of

this controller have been multiplied by a scale factor of 0.1.

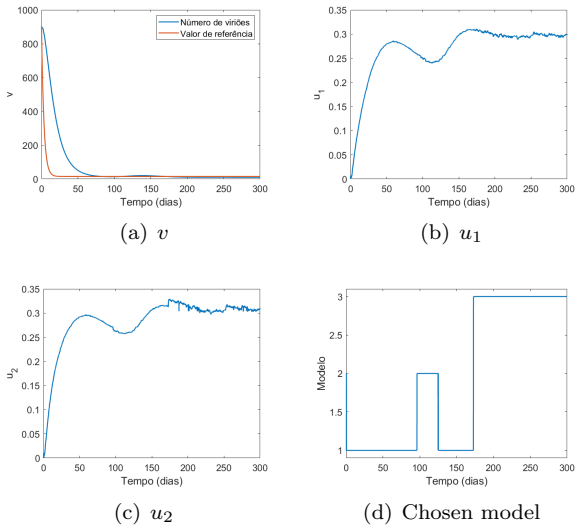

(a) v (b) u_1

(c) u_2 (d) Chosen model

Figure 15: Simulation with multiple model switching.

By observing Figure 15 and comparing the performance of this adaptive control strategy and the case where only a non-adaptive LQ controller is used, no significant improvements are found.

5. Conclusions

The main strength presented in this work is the ability to adapt the controller to the patient in question. As described in section 4 it is possible to estimate the six parameters of the model even when their initial uncertainty is high. With this type of adaptation and using an NMPC controller it will be possible to bring the tracking error to zero in a relatively short time frame. The use of this type of controller also allows the use of a nonlinear cost function which enables an exponential therapy weight that conforms to the actual toxicity values. On the other hand with this controller it will be possible to set a maximum therapy value that can be applied and also to force the control not to oscillate even in cases of high measurement noise by adding two more state variables that penalize sudden therapy variations.

However, this work presents several problems, which implies the need for future work so that it can be applied in a real situation. Firstly, it would be necessary to include a pharmacokinetic and pharmacodynamic model in order to relate the therapy doses taken to the effect values since in this work the control variables used relate to effect values. On the other hand, the patient's descriptor block was always represented by the same three-variable model, thus always representing simulated data. A more real approach would require working with real patient data, which was not possible. Finally, it was always considered that there were new output measures of the patient's values every 6 hours which would be impractical in reality because the common analyzes are done every 3 months. At the limit this data would only be needed every 6 hours at an early stage until the convergence of the parameters and then access to more spaced analysis values.

Acknowledgements

I would like to start by thanking Prof. João Miranda Lemos for this opportunity, for his availability and understanding of the difficulties that were occurring. Prof. João is certainly the person behind most of the ideas in this paper. I would also like to thank my parents and friends for all the help.

References

[1] Introducing HIV/AIDS Education Into the Electrical Engineering Curriculum at the University of Pretoria. *IEEE Transactions on Education*, 47(1):65–73, 2004.

[2] K. Åström. Encyclopedia of Systems and Control. (Bellman 1961):1–9, 2013.

[3] W. Black, P. Haghi, and K. Ariyur. Adaptive Systems: History, Techniques, Problems, and Perspectives. *Systems*, 2(4):606–660, 2014.

[4] S. Bonhoeffer, J. M. Coffin, and M. A. Nowak. Human immunodeficiency virus drug therapy and virus load. *Journal of virology*, 71(4):3275–8, 1997.

[5] S. Bonhoeffer, R. M. May, G. M. Shaw, and M. A. Nowak. Virus dynamics and drug therapy. *Proceedings of the National Academy of Sciences*, 94(13):6971–6976, 1997.

[6] V. Costanza, P. S. Rivadeneira, F. L. Biafore, and C. E. D'Attellis. A closed-loop approach to antiretroviral therapies for HIV infection. *Biomedical Signal Processing and Control*, 4(2):139–148, 2009.

[7] I. Craig and X. Xia. Can HIV/AIDS be Controlled?: Applying control engineering concepts outside traditional fields. *IEEE Control Systems*, 25(1):80–83, 2005.

[8] J. David, H. Tran, and H. T. Banks. Receding Horizon Control of HIV. *Optimal Control Applications & Methods*, 32(6):681–699, 2011.

[9] C. M. Y. T. Denise, Hardt. On The Optimal Doses Of Transcriptase And Protease Inhibitors In The Treatment Of HIV-Seropositive Patients. *7th Portuguese Conference on Automatic Control*, 2006.

[10] J. Hespanha. Tutorial on supervisory control. *Lecture Notes for the workshop Control using Logic and Switching for the 40th Conf. on Decision and Contr.*, pages 1–46, 2001.

[11] S. J. Julier and J. K. Uhlmann. <Julier UhlmannUnscented filtering and nonlinear estimation>. 92(3), 2004.

[12] D. Kirschner, S. Lenhart, and S. Serbin. Optimal control of the chemotherapy of HIV. *Journal of mathematical biology*, 35(7):775–792, 1997.

[13] A. L. Knorr and R. Srivastava. Evaluation of HIV-1 kinetic models using quantitative discrimination analysis. *Bioinformatics*, 21(8):1668–1677, 2005.

[14] J. M. Lemos, J. V. Pinheiro, and V. S. A nonlinear MPC approach to minimize toxicity in HIV-1 infection multi-drug therapy. *10th Portuguese Conference on Automatic Control*, 2012.

[15] P. Oliveira, J. P. Hespanha, J. M. Lemos, and T. Mendonça. Supervised Multi-model Adaptive Control of Neuromuscular Blockade with Off-set Compensation. pages 3064–3069, 2009.

[16] W. H. Organization. Hiv/aids, 2018.

[17] A. S. Perelson and P. W. Nelson. Mathematical Analysis of HIV-1 Dynamics in Vivo. *SIAM Review*, 41(1):3–44, 1999.

[18] J. V. Pinheiro. Design of therapies for hiv-1 infection using predictive control techniques. Master's thesis, Instituto Superior Tcnico, 2011.

[19] H. Shim, S. Han, and C. Chung. Optimal scheduling of drug treatment for HIV infection: continuous dose control and receding horizon control. ... *Journal of Control* ..., 1(3):282–288, 2003.

[20] J. A. M. F. D. Souza, M. Antonio, and L. Caetano. Optimal Control Theory Applied to the Anti-Viral Treatment of AIDS. pages 4839–4844, 2000.

[21] G. Welch, G. Bishop, and C. Hill. An Introduction to the Kalman Filter. pages 1–16, 1997.

[22] H. Wu, Y. Huang, E. P. Acosta, J. G. Park, S. Yu, S. L. Rosenkranz, D. R. Kuritzkes, J. J. Eron, A. S. Perelson, and J. G. Gerber. Pharmacodynamics of antiretroviral agents in hiv-1 infected patients: Using viral dynamic models that incorporate drug susceptibility and adherence. *Journal of Pharmacokinetics and Pharmacodynamics*, 33(4):399–419, Aug 2006.

[23] R. Zurakowski and a.R. Teel. Enhancing immune response to HIV infection using MPC-based treatment scheduling. *Proceedings of the 2003 American Control Conference, 2003.*, 2:1182–1187, 2003.